Decadal Variabilities of the Upper Layers of the Subtropical North Atlantic: An Ocean Model Study

TAL EZER

Program in Atmospheric and Oceanic Sciences, Princeton University, Princeton, New Jersey

(Manuscript received 13 July 1998, in final form 8 February 1999)

ABSTRACT

Numerical simulations of the Atlantic Ocean during the period 1950 to 1989, using a sigma coordinate, free surface numerical model, show long-term variabilities in the upper ocean subtropical gyre similar to those obtained from observations. The simulations show how westward propagating planetary waves, originated in the eastern North Atlantic, affect interdecadal variabilities of ocean properties such as the Bermuda sea level, the Gulf Stream position and strength, and subsurface temperature anomalies in the western North Atlantic. Special attention is given to the dramatic sea level drop at Bermuda in the early 1970s, which is accompanied by cooling of subsurface layers in the western North Atlantic and a northward shift and weakening of the Gulf Stream. Following these events, between 1970 and 1980, the cold temperature anomalies in the upper layers of the western North Atlantic slowly propagated eastward and downward; the strongest propagating signal in the model is found at 200-m depth, suggesting that advection of anomalies downstream by the Gulf Stream current and changes in winter mixing are involved. Significant correlations were found between the sea level anomalies at Bermuda and sea level anomalies in the eastern North Atlantic up to eight years earlier. Sensitivity experiments with different atmospheric forcing fields are used to study the ocean response to observed sea surface temperature and wind stress anomalies. It is shown that on decadal timescales, the ocean model responds in a linear fashion to the combined effect of SST and wind stress anomalies, a fact that might be exploited in future climate prediction studies.

1. Introduction

Long-term variations in the Atlantic Ocean may be important for possible climatic changes and thus have been the subject of considerable recent research using long-term observations (e.g., Kushnir 1994; Levitus et al. 1994; Molinari et al. 1997), diagnostic and prognostic ocean models (e.g., Greatbatch et al. 1991; Ezer et al. 1995; Häkkinen 1995; Halliwell 1998), and coupled ocean–atmosphere models (e.g., Delworth et al. 1993; Griffies and Bryan 1997; Grotzner et al. 1998; Latif 1998). It is generally believed that, on shorter-term interannual timescales, the atmosphere drives ocean variability, in particular sea surface temperature (SST) anomalies, while on longer-term interdecadal timescales, variations in the thermohaline ocean circulation drives atmospheric changes, and in fact, North Atlantic SST anomalies correlate with climatic changes in wind patterns on decadal timescales as shown by Kushnir (1994). However, the recent study of Halliwell (1997, 1998) suggests that, even on decadal timescales, local atmospheric forcing may play a more important role in oceanic changes than previously realized. Although interdecadal and decadal climate variabilities involve the two-way ocean–atmosphere interaction (see for example the recent review of this problem by Latif 1998), ocean-only models, nevertheless, can still be useful tools to study the response of the ocean to atmospheric variability. An important question is whether or not an ocean model can produce some of the observed subsurface interdecadal variabilities (Levitus 1989; Levitus et al. 1994; Molinari et al. 1997) given only surface data.

The problem of understanding Atlantic climate variability involves many complex processes that are beyond the scope of this study, such as ocean–atmosphere feedback, sea–ice interaction, and deep-water formation in high latitudes; here we focus only on one aspect of the long-term variability: decadal changes in the upper subtropical gyre and their relation to surface forcing and to long Rossby waves. Westward propagating, baroclinic, long Rossby waves (or planetary waves) have been well known to oceanographers for many years (e.g., LeBlond and Mysak 1978), but only more recently, with the development of satellite altimetry technology, they have been globally observed (e.g., Chelton and Schlax 1996) and compared with models (Stammer and Wunsch 1994; Semtner 1995; Cipollini et al. 1997; Fu and Smith 1996;

Corresponding author address: Dr. Tal Ezer, Program in Atmospheric and Oceanic Sciences, Princeton University, Post Office Box CN710, Sayre Hall, Princeton, NJ 08544-0710.
E-mail: ezer@splash.princeton.edu

© 1999 American Meteorological Society

Killworth et al. 1997). These waves, which propagate at speeds of a few centimeters per second, play an important role in the low frequency variability of the ocean and the dynamics of low and middle latitudes.

Our investigation has been largely motivated by the study of Sturges and Hong (1995) who used a simple wind-driven Rossby wave model described by the product of pressure and the *n*th vertical mode eigenfunction, $p_n(x, y, t)F_n(z)$, satisfying the equation

$$\frac{\partial p_n}{\partial t} - C_n \frac{\partial p_n}{\partial x} = B_n \,\mathrm{curl}(\tau/\rho_o f), \qquad (1)$$

where τ is the wind stress, ρ_o is a reference density, f is the Coriolis parameter, B_n is proportional to the integral of the vertical mode over the mixed layer depth, and C_n is the phase speed calculated for each mode from hydrographic observations [see Sturges and Hong (1995) and Sturges et al. (1998) for detail]; in these studies, the first two baroclinic modes explain most of the observed variability. This model has been used to study the propagation of waves in the subtropical gyre (Sturges et al. 1998) and the variability of the coastal sea level along the U.S. East Coast (Hong et al. 1998, manuscript submitted to *J. Phys. Oceanogr.*), wherein the wind-driven open ocean wave model of (1) was linked to a simplified Gulf Stream transport model. This simple model shows very good agreement with observed long-term sea level changes at Bermuda (Sturges and Hong 1995), so we were intrigued in seeing if a more complete three-dimensional model that includes many processes, not included in (1), can capture the observed changes as well. In a three-dimensional model of the type used here, the Gulf Stream is, of course, an integral part of the prognostic solution and thus the simulations will allow us to see whether or not the assumptions made in the simple model are valid and if long-term Gulf Stream variabilities are related to long Rossby waves.

The main goal of the study is to evaluate if an ocean model can produce the observed decadal variabilities in the ocean given observed atmospheric anomalies and to further investigate the processes involved in the long-term variabilities of the subtropical North Atlantic.

The paper is organized as follows: First, in section 2, the ocean model and the experiments are described; then in section 3, the decadal variabilities of the subtropical gyre in the model simulations are presented; and finally, discussion and conclusions are offered in section 4.

2. The ocean model and the experiments

The earliest ocean models and coupled ocean–atmosphere models used for climate studies were based on different versions of the *z*-level Bryan–Cox model (Bryan 1969) and its successor, the Modular Ocean Model (MOM), developed at the Geophysical Fluid Dynamics Laboratory. More recently, isopycnal models have been also tested for climate simulations (Oberhuber 1993; New and Bleck 1995; Halliwell 1998); see Chassignet et al. (1996) for a comparison between the two types of models. The Princeton Ocean Model (POM: Blumberg and Mellor 1987) on the other hand, had previously been used mostly for coastal and regional applications. However, POM is now also being used for climate studies in basin-scale domains (Ezer and Mellor 1994, 1997; Häkkinen 1995; Ezer et al. 1995; Mellor and Ezer 1995). The use of a free surface, bottom following sigma-coordinate system and a submodel for turbulent mixing (Mellor and Yamada 1982) in POM is attractive in studying processes such as surface and bottom boundary layer dynamics, deep-water formation, and flows over sills, which are important for climate simulations. An application of POM to the entire Atlantic Ocean, with the same model configuration as used here, shows an intense deep western boundary current and quite realistic meridional overturning circulation and meridional heat flux (Ezer and Mellor 1997). The latter study (hereafter EM97) was the first time that this type of a model has been implemented for the entire Atlantic Ocean and executed for many years. The model climatology when forced with monthly mean climatological SST and wind stress is discussed in detail by EM97; here the goal is to further test the model characteristics when interannual and interdecadal anomalies in surface data are also taken into account (seasonal variabilities are included in both, the climatological and the interannual simulations). The Atlantic Ocean model configuration and boundary conditions are exactly as in EM97. The model grid and the bottom topography are shown in Fig. 1; the curvilinear orthogonal grid has variable resolution with a typical grid size of 50–100 km (with higher resolution in the Gulf Stream and the Antarctic Circumpolar Current regions). The variable grid size allows one, for example, to crudely represent the Florida Straits with three to four grid points. While the model resolution is not eddy resolving (e.g., the grid size in the Gulf Stream area is slightly larger than the radius of deformation there), it is generally higher than many climate models. For the large-scale processes studied here, higher resolution models may not be crucial, though they may add more detail to the Gulf Stream response, so we do plan to test higher resolution models in the future. The bottom following 16 sigma layers are distributed such that higher resolution is used near the surface and lower resolution in the deep layers (see EM97 for details). Since the study focuses on the subtropical North Atlantic region, the area of interest is removed from unwanted influence of open lateral boundary conditions.

To test the model response to variations in surface forcing, four simulations are performed:

1) experiment E0—forced by monthly mean climatological SST and wind stress;
2) experiment E1—same as E0, but with additional monthly wind stress anomalies;

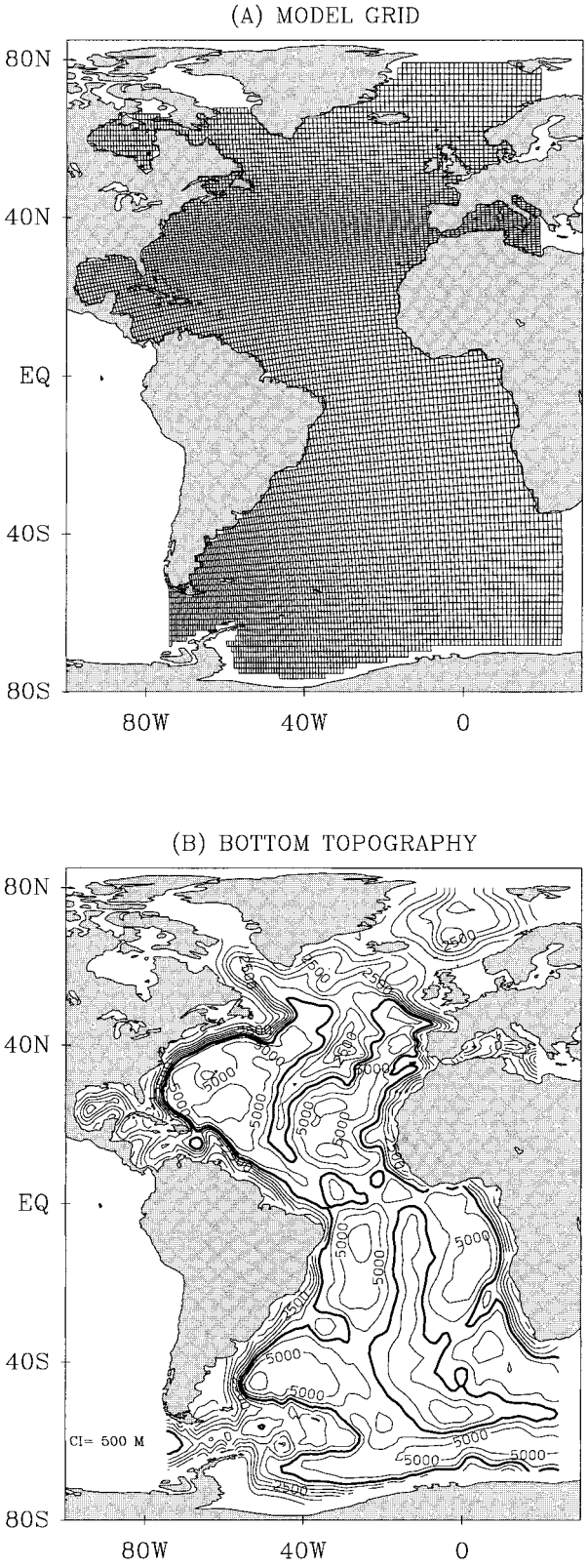

FIG. 1. (a) Curvilinear orthogonal model grid and (b) bottom topography. Contour interval in (b) is 500 m; the 4000-m isobath is indicated by a heavy line.

3) experiment E2—same as E0, but with additional monthly SST anomalies; and
4) experiment E3—includes both SST and wind stress monthly anomalies.

Therefore, the surface forcing in E0 includes only the mean annual cycle, while the surface forcing in E1, E2, and E3 includes additional interannual variations in the wind, SST or both. For example, in E2 and E3 the SST forcing is the monthly mean values plus the anomaly, $\langle \mathrm{SST}(x, y, \mathrm{month}) \rangle + \Delta\mathrm{SST}(x, y, \mathrm{month}, \mathrm{year})$, where angle brackets represent a 40-yr time mean and delta represents the monthly anomaly relative to the mean. Surface salinity is held fixed and equal to the annual climatology of Levitus (1982) so that seasonal and interannual variations in surface salinity are ignored in these experiments. Such variations may be important for deep-water formation in high latitudes and long-term thermohaline circulation changes (Weaver et al. 1991), but we did not see any significant effect on the subtropical variations discussed here when seasonal surface salinity changes are included in the calculations. The surface wind stress and surface temperature data (climatologies and anomalies) are derived from the Comprehensive Ocean–Atmosphere Data Set (COADS) analyzed by da Silva et al. (1994); the analysis was obtained from data collected over the period 1945 to 1989, but results will be shown only for the period starting in 1950.

All the experiments start from the same initial condition (Levitus 1982) and use the same lateral boundary conditions; they differ only by the different surface forcing. The first 30 years of experiment E0 is the climatological simulation of EM97. In experiments E1, E2, and E3 surface anomalies are imposed after a 10-yr spinup with climatological forcing. Although adjustment of the deep ocean may require a much longer spinup period (which may not be computationally possible with the type of model used here), for the upper-ocean processes studied here the simulations of EM97 show a complete ocean adjustment within 10 years. A small, but nonnegligible model climate drift exists in the model as shown in EM97; however, it is assumed that the model climate drift is the same in all experiments; it will be removed based on the climate drift of E0. Since the model climate drift is monotonic and is decaying with time, it is easily distinguished from the oscillatory nature of the decadal variabilities discussed here.

As discussed in EM97, the SST and the surface salinity are used directly as the surface boundary condition. This may reduce the variability of the thermohaline circulation compared to the use of heat fluxes (Seager et al. 1995), and, in fact, with climatological forcing (as in E0), interannual variabilities are quite small. However this situation is actually convenient for our sensitivity studies since subsurface changes in experiments E1–E3, if they exist, can be more easily identified with variations in surface conditions.

3. Model results

a. Surface and subsurface variations in the western North Atlantic and the Gulf Stream

Although the model domain (Fig. 1) covers the entire Atlantic Ocean, in this study we consider only the region from the equator to middle latitudes; the 40-yr-long mean and variability obtained from experiment E3 are shown for this region in Fig. 2. For a model of this resolution, the mean surface elevation field and the Gulf Stream separation (Fig. 2a) are fairly realistic. The root-mean-square (rms) of the monthly mean elevation anomalies (Fig. 2b) shows maximum values in the Gulf Stream region, owing to seasonal and interannual variabilities. The maximum value, almost 10 cm, is smaller compared to the Gulf Stream mesoscale variabilities (where rms ≈ 30 cm) as obtained from regional and global high-resolution models and from altimeter data (e.g., Ezer and Mellor 1994; Stammer and Wunch 1994; Semtner 1995). The level of variability shown in Fig. 2b is comparable to the variability associated with the annual cycle as obtained from TOPEX/Poseidon altimeter (Fu and Smith 1996). When the surface elevation of the 40-yr simulation is filtered (a cosine squared filter is used here and in the following analyses) to remove periods shorter than 2 yr, the spatial distribution of the variability is much different than that of the seasonal and interannual variabilities (Fig. 2c). Two areas where variability is relatively large are the middle and high latitudes, north of 40°N, and the western portion of the subtropical gyre. The variability in high latitudes is associated with the interdecadal wind shift in those latitudes owing to the North Atlantic oscillation (NAO) (Kushnir 1994; Hurrell 1995); the focus of our study, however, will be mostly on the variability in the subtropical gyre.

The filtered wind stress anomalies and SST anomalies, averaged over the latitudinal band between 25°N and 35°N, are shown in Figs. 3 and 4a, respectively. Decadal oscillations are most apparent in the zonal wind stress (Fig. 3a) and to lesser extent in the amplitude (Fig. 3c). The variations follows the NAO index (defined by Hurrell 1995 as the sea level pressure difference between Portugal and Iceland), with more eastward (positive values in Fig. 3a) wind anomalies during periods of low NAO index (e.g., 1969, 1978) and more westward wind anomalies during periods of high NAO index (e.g., 1967, 1974, 1983); decadal variations of this nature have been described before (Kushnir 1994). While the anomalies in the zonal wind stress do not show any indication of signal propagation, the meridional component (Fig. 3b) and the curl of the wind stress (Fig. 3d) do show one case of possible westward propagating signal during the 1960s. The pattern of negative wind stress curl anomaly has some resemblance to the pattern of negative SST anomaly (Fig. 4a), especially during the 1960s and 1970s. Figures 4b–d show the model (expt. E3) subsurface temperature anomalies. An outstanding feature in the subsurface temperature is the strong cooling seen at 100-m depth around 1970. The cold anomaly seems to slowly propagate eastward at deeper layers between 1970 and 1985 (Figs. 4c and 4d). McCartney et al. (1997) suggest a possible mechanisms

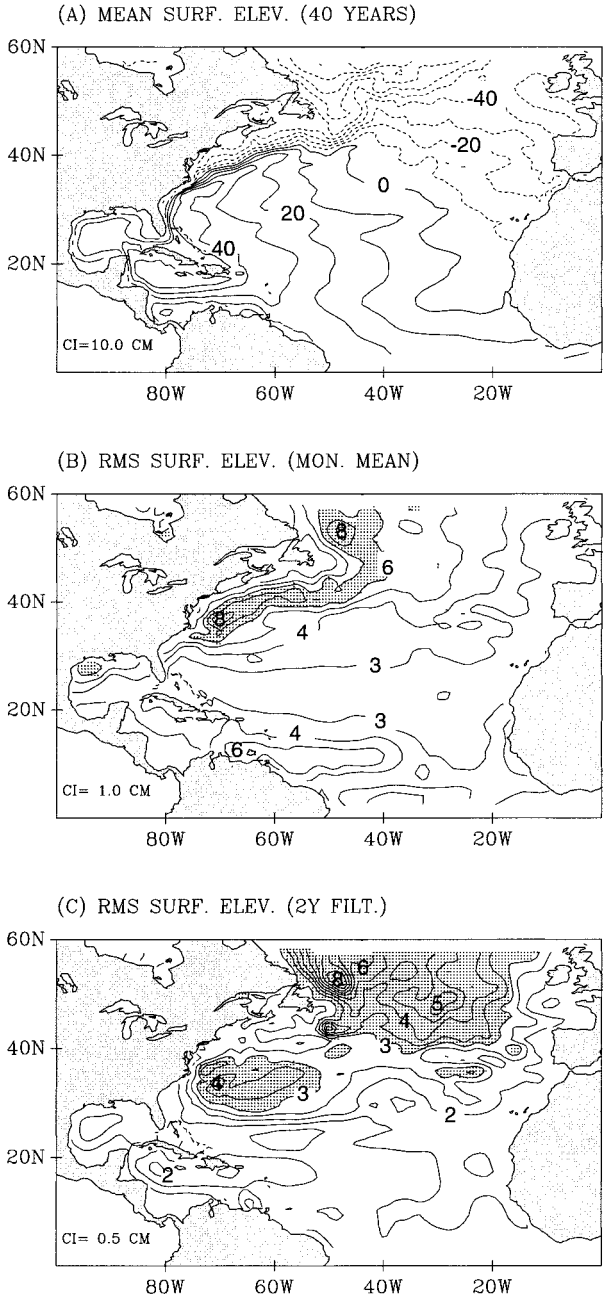

FIG. 2. Mean and variability of the subtropical and middle latitude portion of the model shown in Fig. 1, calculated from a 40-yr integration of expt. E3. (a) Mean surface elevation; contour interval is 10 cm, dashed contours represent negative values. (b) Rms surface elevation anomaly calculated from monthly mean values; contour interval is 1 cm, shaded areas represent values larger than 6 cm. (c) Rms surface elevation anomaly calculated from values filtered to remove periods shorter than 2 yr; contour interval is 0.5 cm, shaded areas represent values larger than 3 cm.

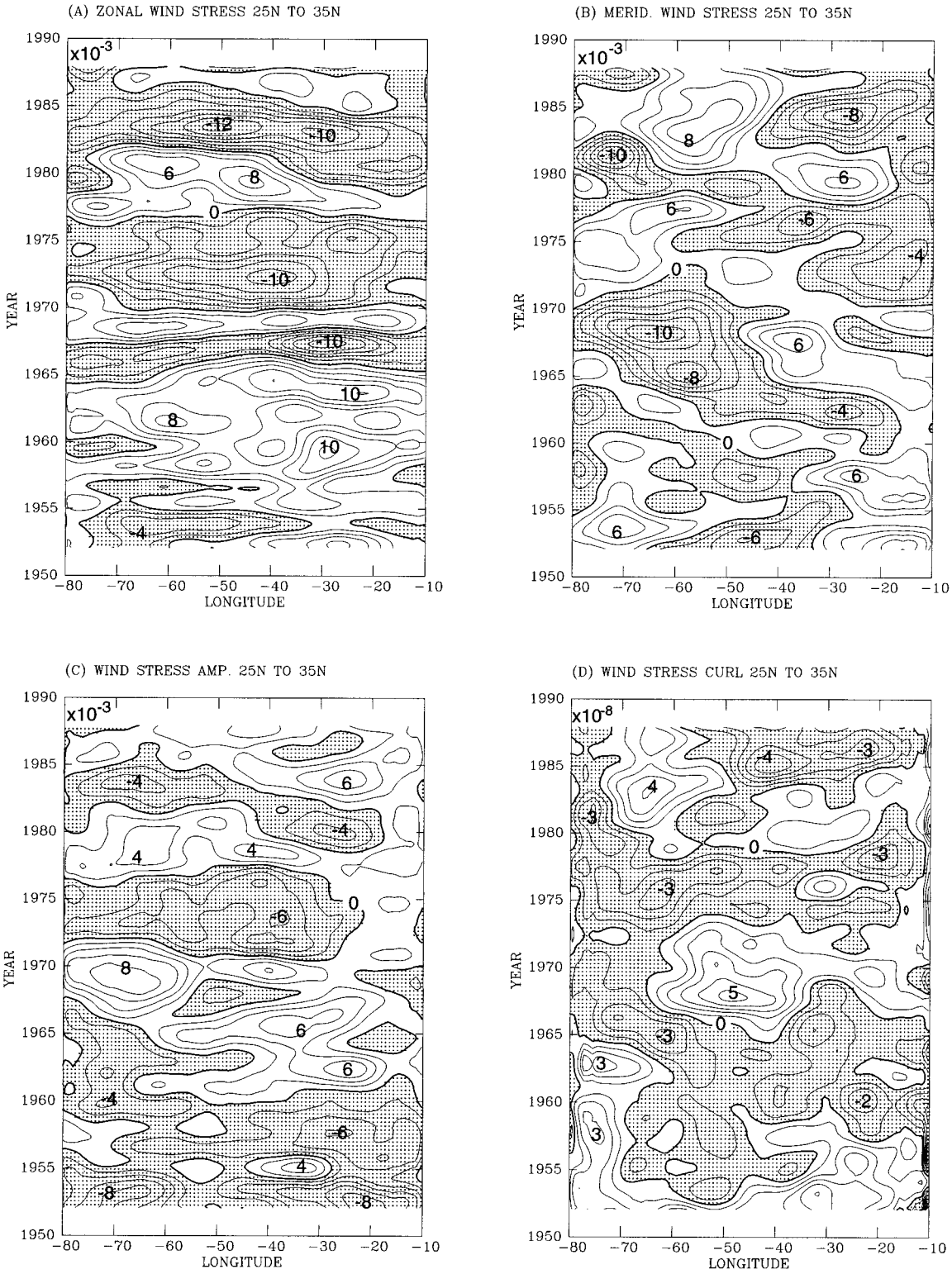

FIG. 3. Variability of COADS wind stress fields as a function of longitude and time; the data were averaged over the latitude band 25° to 35°N and filtered to remove periods shorter than 2 yr. (a) Anomaly of the zonal wind stress component, τ_x. (b) Anomaly of the meridional wind stress component τ_y. (c) Anomaly of the wind stress amplitude $|\tau|$. (c) Anomaly of the wind stress curl curl(τ). Shaded areas represent negative values; contour intervals are 0.002 N m^{-2} in (a)–(c) and 10^{-8} N m^{-3} in (d).

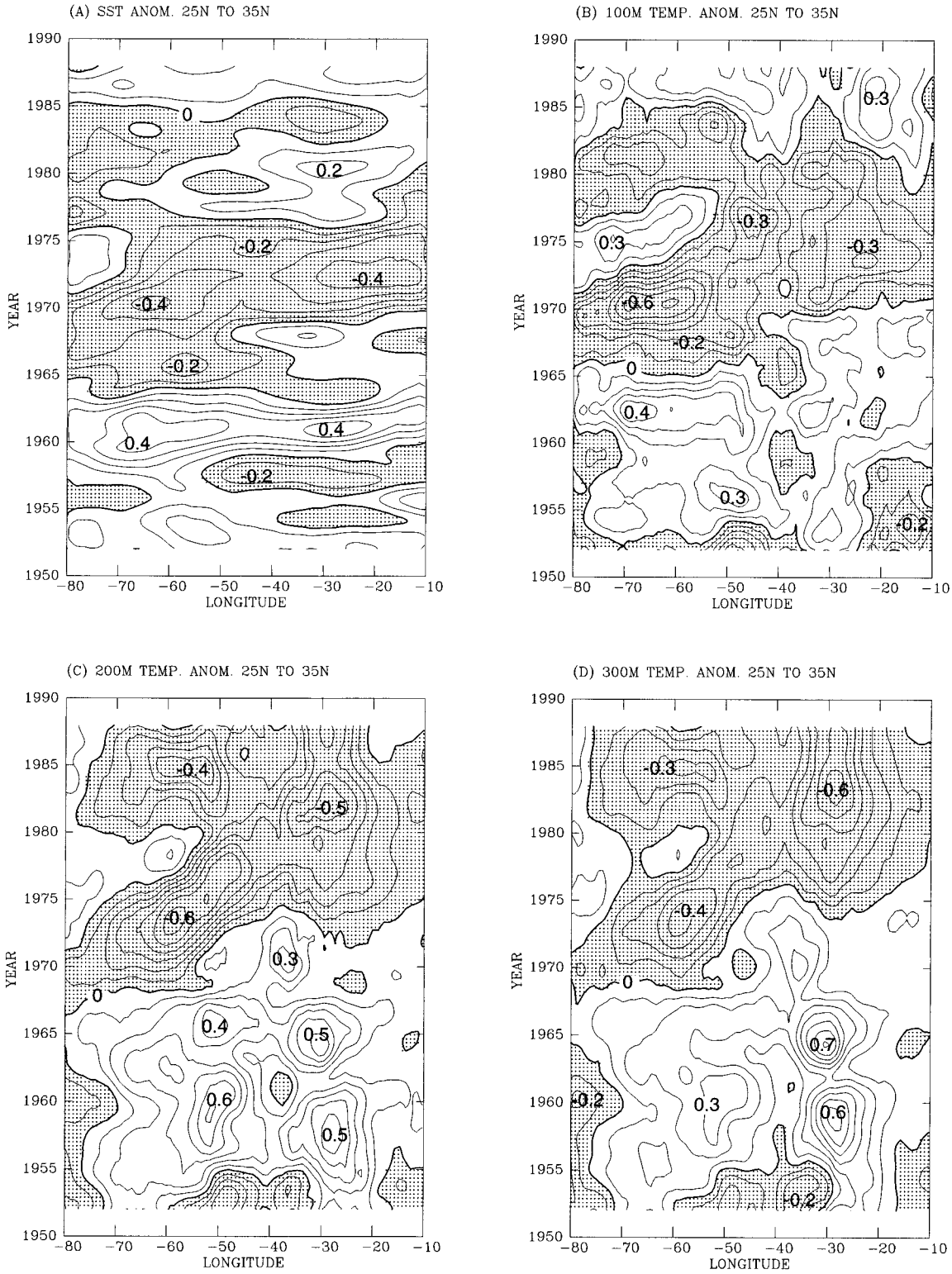

FIG. 4. Model temperature anomaly as a function of longitude and time in expt. E3; the data were averaged over the latitude band 25° to 35°N and filtered to remove periods shorter than 2 yr. (a) At the surface, (b) at 100-m depth, (c) at 200-m depth, and (d) at 300-m depth. Shaded areas represent negative values; contour intervals are 0.1°C.

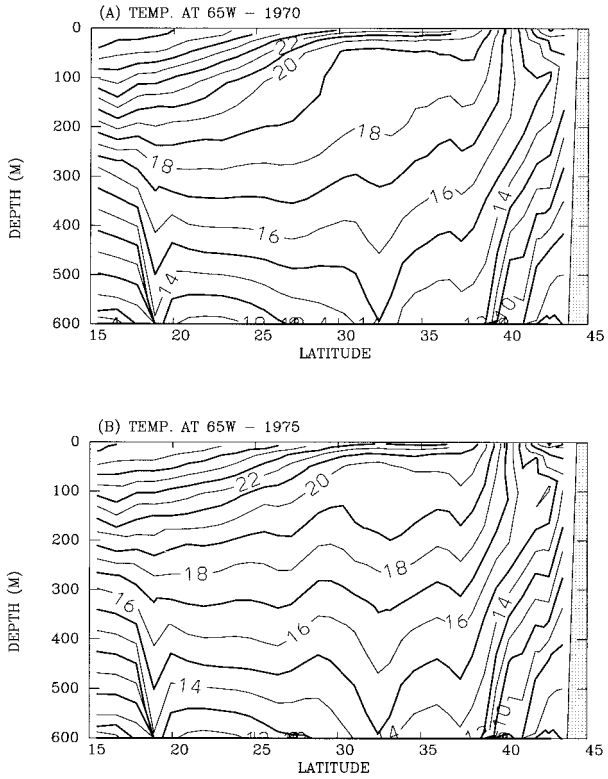

FIG. 5. Annual mean temperature at a cross section in the upper ocean (expt. E3) along 65°W from 15° to 45°N, (a) for 1970 and (b) for 1975. Contour interval is 1°C.

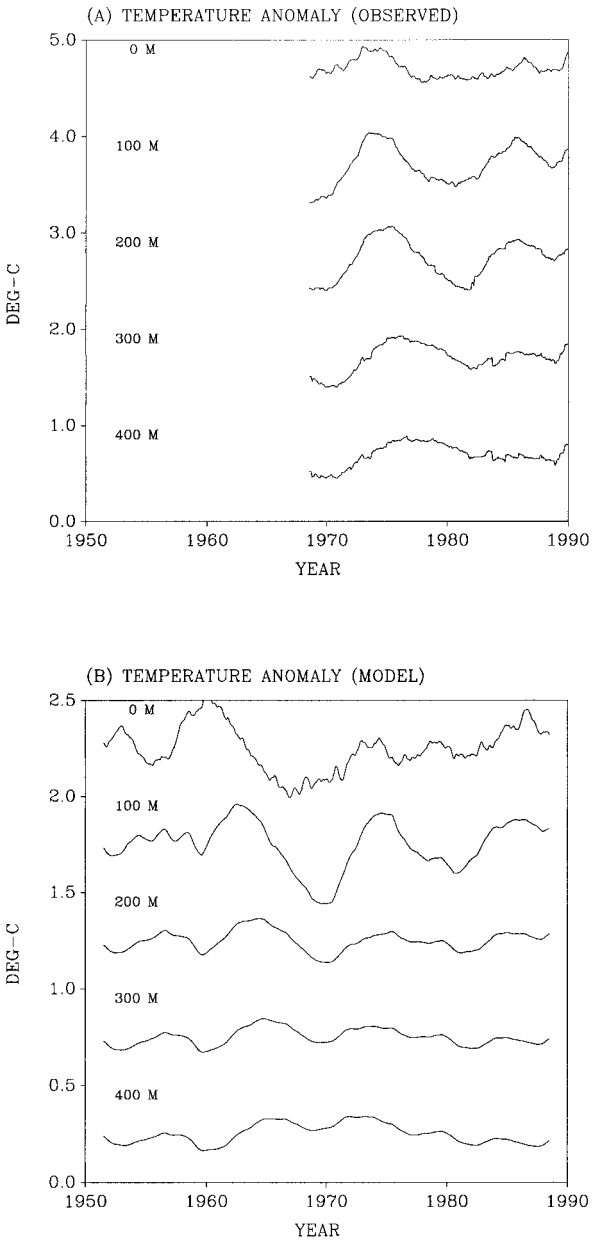

FIG. 6. Area averaged temperature anomaly in different depths (as indicated) calculated over the western North Atlantic (17° to 43°N, 78° to 66°W). (a) The analyses obtained from expendable bathythermograph (XBT) observations taken between 1966 and 1995 and presented by Molinari et al. (1997). (b) Model results (expt. E3). The mean of each line has been shifted for clarity; the vertical axis is shown for scaling purpose only. Note the different scale of (a) and (b). A 3-yr running average has been applied to the time series of each depth.

that involves downstream propagation of anomalies (by the eastward flowing Gulf Stream in our case) and interaction with the atmosphere, which causes changes in winter mixing at downstream locations; the result is a very slow propagation of SST anomalies as shown for example by Hansen and Bezdek (1996). That subsurface propagating temperature anomalies have amplitudes larger than the surface anomalies suggests that the signal originated in the subsurface layers of the subtropical gyre. Therefore, to further investigate those subsurface changes, north–south cross sections of temperature across the Gulf Stream at 65°W are shown for a year with colder SST, 1970 (Fig. 5a), and for a year with warmer SST, 1975 (Fig. 5b). The most noticeable change between those years is the upward lifting of isotherms at middepth during 1970 compared with 1975. For example, the 19°C isotherm at 33°N is more than 150 m higher in 1970 than in 1975 resulting in colder waters at depth between 100 and 200 m, as seen in Fig. 4. The homogenized water mass (the so-called ''18 degree water'') is larger in volume during 1970, suggesting that the change in the middepth thermal structure during the period of cold SST results from more intense winter subduction.

Recent analysis by Molinari et al. (1997) of temperature data from 1966 to 1995 in the western North Atlantic between 17° and 43°N, 78° and 66°W shows clear interdecadal variations in the upper 400 m of the ocean; the maximum amplitude of those variations are found around 100-m depth with decreasing amplitudes at the surface and at greater depths (Fig. 6a reproduces the part of the data presented in Molinari's paper that overlaps our simulations). The later variations also correlate

with the NAO index. To test whether or not the model exhibits variations similar to those obtained from observations, the area-averaged temperatures in the western North Atlantic have been calculated and shown in Fig. 6b [the area and the depths chosen are as in Molinari et al. (1997, Fig. 2) but the time period is different, so the means and the trends that were removed from the records to calculate the anomalies are different]. The observed and model temperature records have been filtered with a 3-yr running average to remove high-frequency variations. The model results show interdecadal variations similar to those observed with maximum amplitude around 100 m; the results also indicate propagation of the signal downward with time, as in the observed record. The positive anomalies at 100-m depth during the mid 1970s and mid 1980s and the cold anomaly in the early 1970s coincide with the observed anomalies discussed by Molinari et al. (1997). However, the amplitudes of the variations of subsurface temperatures in the model are underestimated by a factor of 2 in comparison with the observations (note the change in scale between Fig. 6a and 6b). This discrepancy between the model results and the observations can be partly attributed to the discrepancy between the COADS SST used to force the model (the upper line in Fig. 6b) and the local observations used by Molinari et al. (1997). Since the COADS analysis is based on monthly and spatial ($1° \times 1°$) averages, the variations in COADS SST are generally smaller than those of local observations with higher temporal and spatial resolution. Additional model errors, such as too much diffusion, can also contribute to the underestimation of subsurface model changes. The model calculations for the period preceding the observations indicate variations of similar nature to those observed in the more recent period. For example, the pronounced warm anomaly during the middle 1960s is indicated by an SST anomaly around 1962 and reached 400-m depth around 1966.

The mean Gulf Stream surface slope and axis position (i.e., the location of the maximum slope) are calculated from all the model grid lines that cross the Gulf Stream between 60° and 75°W and shown in Fig. 7. The abrupt changes in the strength of the Gulf Stream (i.e., the surface current relates to the surface slope) during the early 1970s seem to be coherent with abrupt changes in the position of the Gulf Stream axis. For example, a northward shift in the Gulf Stream axis around 1970 corresponds to weakening of its flow and the latter leads the former by 1–3 years. Our results corroborate previous observations and diagnostic calculations of the interpentadal changes between 1955–59 and 1970–74. For example, between the two pentads a drop in sea level at Bermuda and an increase in sea level along the U.S. East Coast (Levitus 1990; Ezer et al. 1995) results in decreasing sea level slope across the Gulf Stream as seen in Fig. 7. Diagnostic calculations (Greatbatch et al. 1991; Ezer et al. 1995) also suggest that the Gulf Stream strength may have weakened by as much as 30%

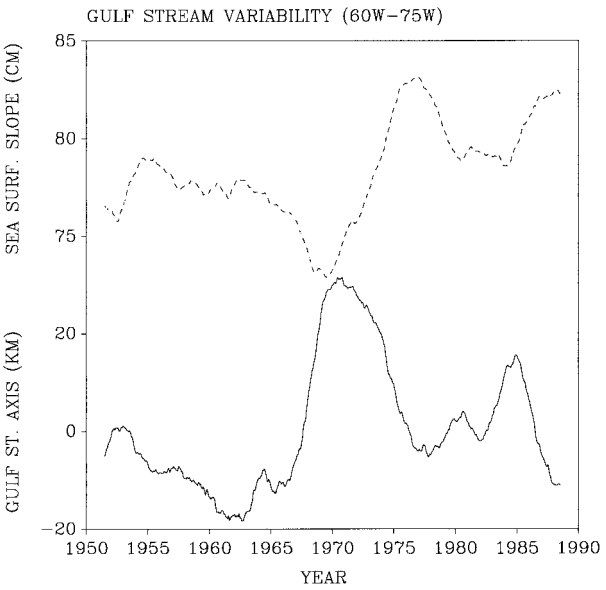

FIG. 7. Spatial mean Gulf Stream north–south axis shift and surface slope calculated from all model grid lines crossing the Gulf Stream between 60° and 75°W. Solid line is the Gulf Stream axis anomaly in km (positive values indicate northward position relative to the long-term mean position), dashed line is the average sea surface difference across the Gulf Stream in cm (which corresponds to the strength of the surface current).

between the late 1950s and the early 1970s. Our prognostic model results produce a weakening of about 15% in the upper Gulf Stream flow during the same period; the weakening of the Gulf Stream total transport is also of similar percentage (not shown). According to the Gulf Stream separation study of Ezer and Mellor (1992), weakening of the northern recirculation gyre of the Gulf Stream is correlated with a northward shift in the Gulf Stream axis; therefore, the weakening of this gyre during the early 1970s (Greatbatch et al. 1991; Ezer et al. 1995) may be related to the northward shift seen in Fig. 7. There is also a clear similarity between the shift of the Gulf Stream axis in Fig. 7 and the changes in the 100-m temperature anomaly in Fig. 6. Figure 5 further suggests that cooling of the subsurface water mass in the subtropical gyre south of the Gulf Stream during 1970 degrades the thermal front across the Gulf Stream and thus causes a weaker Gulf Stream as seen in Fig. 7.

b. The Bermuda sea level change and long planetary waves

We next look closely at sea level changes at Bermuda where a long-term sea level record exists. Our interest in the Bermuda sea level has been largely motivated by the study of Sturges and Hong (1995). In that study, a simple, wind-driven Rossby wave model (1), driven only by COADS wind stress curl, was able to produce the observed interdecadal changes of sea level at Bermuda with amazing accuracy, suggesting that local

wind-driven Ekman pumping and remote planetary waves account for much of the Bermuda sea level change. Figure 8a compares the observed sea level change in Bermuda to the Sturges and Hong model and to results of experiment E3; the annual cycle and short-term interannual variabilities have been filtered out from all records. The two model sea levels compare quite well with the observed sea level; in particular, they produce the large sea level drop around 1970. Figure 8b compares the experiments E1, E2, and E3 to the observed record. Some of the long-term sea level changes have been simulated when only SST anomalies (E2, dotted line) or only wind anomalies (E1, dashed line) are taken into account; however, it is clear that both SST and wind anomalies are needed (as in E3) to account for the observed sea level change in 1970. The results invite two intriguing questions: First, what is the reason for the slightly better performance of the simple model of Sturges and Hong (1995) over the three-dimensional model and, second, why does the three-dimensional model require SST anomalies forcing? As to the first question, one should keep in mind that while the three-dimensional model is more complete and includes additional processes such as mixing and thermodynamics that are ignored in the simple model, it also includes numerical errors (for example, uncertainties in the parameterization of subgrid-scale processes and diffusion) that may amplify errors in the forcing, topography, or lateral boundary conditions. For a process dominated by a long-term wind-driven signal such as seen in the filtered Bermuda sea level signal (after short-term variations are removed), one may argue that the simple model should suffice. However, more complete models are required to study variations in the ocean stratification, horizontal circulation, thermohaline overturning circulation, or other processes that are ignored in a simple model based on (1). As to the second question, the answer lies in the way surface forcing is imposed in the model. Since the three-dimensional model includes thermodynamics, it requires using either SST or heat flux surface forcing data; in our case, SST is used as surface forcing. When SST anomalies are ignored (as in E1), monthly mean SST values are imposed at the surface, constraining changes in the thermal structure of the upper ocean and allowing only direct wind-driven sea level changes. On the other hand, when surface heat flux is

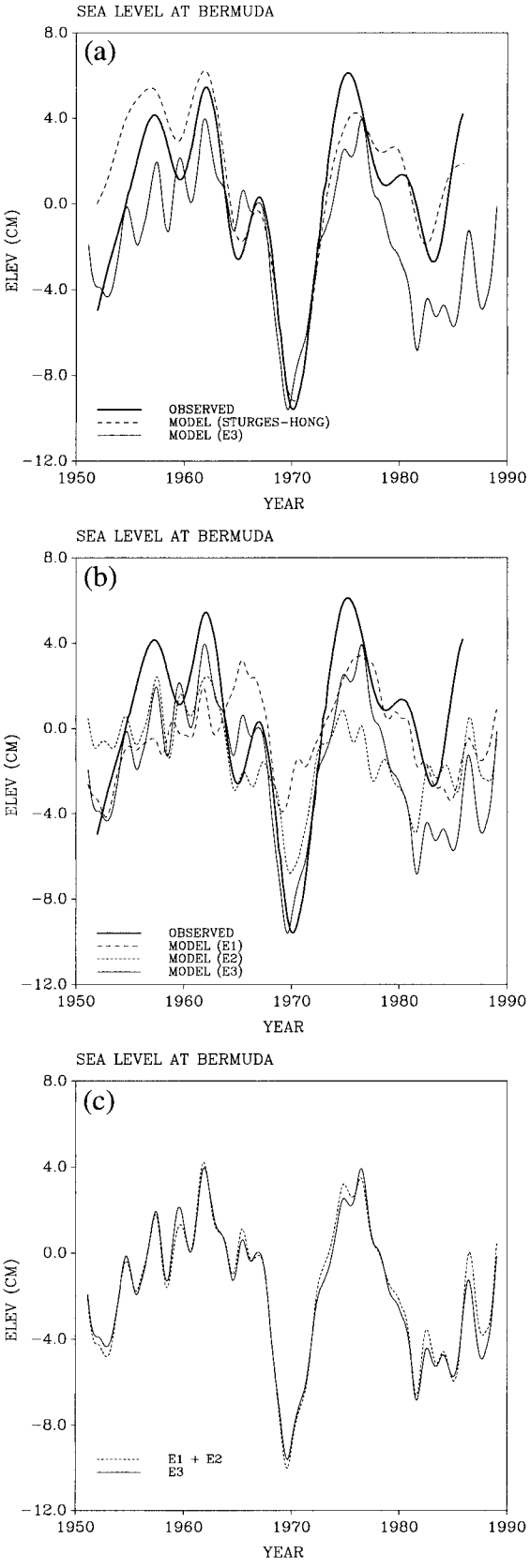

→

FIG. 8. Sea level at Bermuda. The data have been filtered to remove seasonal and high frequency variations. (a) Comparison between the observed sea level (solid heavy line), the model calculations of expt. E3 (narrow solid line), and the calculations of the model of Sturges and Hong (1995) (dashed line). (b) Comparison between the observed sea level (solid heavy line) and model sea level from expts. E1 (dashed line), E2 (dotted line), and E3 (narrow solid line). (c) Comparison between the sum of the changes of expts. E1 and E2 (dotted line) where wind anomalies or SST anomalies are used separately and expt. E3 (solid line).

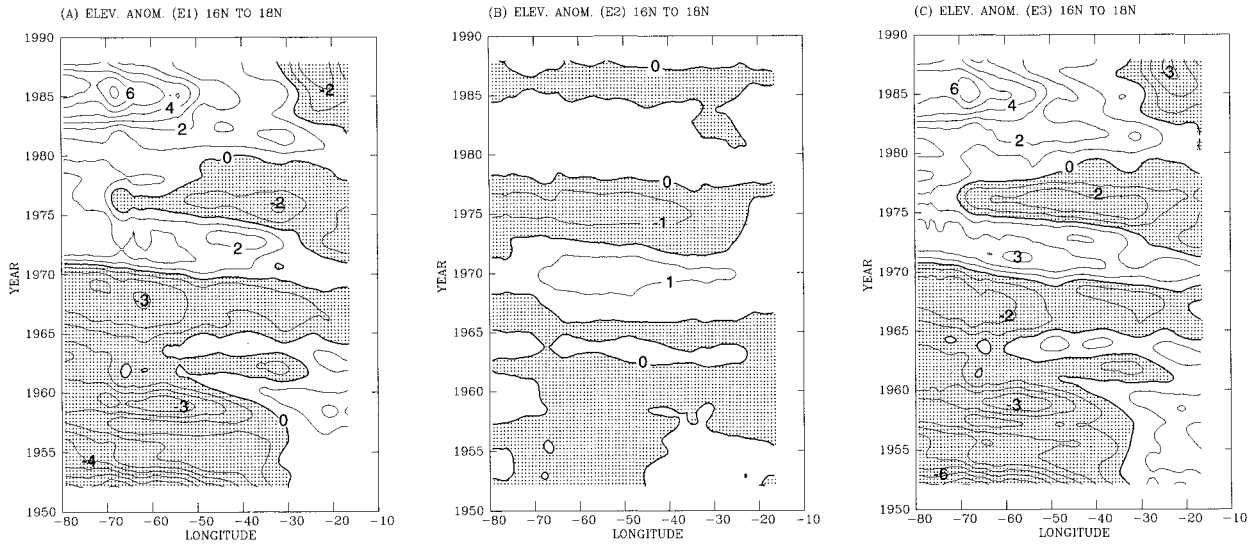

FIG. 9. Surface elevation anomaly as a function of longitude and time averaged for the latitude band 16° to 18°N for expts. (b) E1, (b) E2, and (c) E3. Contour interval is 1 cm, shaded areas represent negative values.

used as a boundary condition, SST is a prognostic variable of the model. Since there are no reliable observations of the long-term variations of the surface heat flux, in this case the heat flux needs to be calculated from the wind and other atmospheric parameters (e.g., Seager et al. 1995). While the latest approach has some advantages over boundary conditions that impose SST, in such an approach it will be more difficult to distinguish between the wind-driven and the SST-driven response as done here where SST and wind forcing are treated as two independent forcing fields. In any case, the fact that the two very different models produce quite a similar long-term response and long Rossby waves with comparable amplitudes and phases is interesting to note.

To further investigate the relation between the SST- and wind-forced response on decadal time scales in the model, we show in Fig. 8c a comparison between the sea level change of E3 and the sum of the sea level changes of E1 and E2 (where wind or SST anomalies are taken into account separately). The comparison is extremely good. The interpretation of this result is that the combined response of the ocean model to SST and wind stress anomalies on decadal timescales is very linear. This interesting result may not be completely surprising since the interdecadal surface anomalies are very small compared with the mean forcing fields.

We next look at the nature of surface elevation anomalies in our model beyond Bermuda to see if propagation of surface anomalies can be identified, where do they occur, and how do they relate to the atmospheric forcing. Figures 9–12 show the longitude versus time plots of filtered surface elevation anomalies obtained from the different experiments and averaged over different latitude bands. In lower latitudes, the patterns of the anomalies in experiment E1, which uses only wind anomalies as forcing (Figs. 9a and 10a), closely resemble the patterns in E3 (Figs. 9c and 10c); much smaller elevation anomalies exist in E2, which uses only SST anomalies as forcing. This result implies that at the tropical and subtropical regions the simulated anomalies are mostly wind driven. In contrast, at middle and higher latitudes the opposite is true so that the results of E2 closely resemble the results of E3 (cf. Figs. 11b to 11c and 12b to 12c), an indication that at middle latitudes the decadal anomalies in the model are more influenced by SST anomalies than by wind anomalies. An interesting exception is the Gulf Stream region (the area west of 70°W in Fig. 11), which is mostly wind driven. This result is in agreement with the model of Halliwell (1998) who concludes that SST anomalies in the Gulf Stream were associated with changes in the wind-driven subtropical gyre circulation; this assumption was also the basis for the simple coastal model of Hong et al. (1998, manuscript submitted to *J. Phys. Oceanogr.*).

The most prominent feature in the surface elevation anomaly in Fig. 11c is the negative anomaly between 60° and 70°N around 1970, which occurs around the same time as the subsurface temperatures were anomalously cold, the Gulf Stream had shifted northward, and the Bermuda sea level had dropped, as discussed before. In the period preceding these strong events Fig. 12c indicates a westward propagation of negative surface anomaly originating from the northern eastern Atlantic around 1963 and reaching the western Atlantic around 1967; this is the strongest anomaly found at this latitude during the entire 40 years integration. This anomaly later propagated eastward during the 1970s. At the same time, near the southern portion of the subtropical gyre, one can also see westward propagating

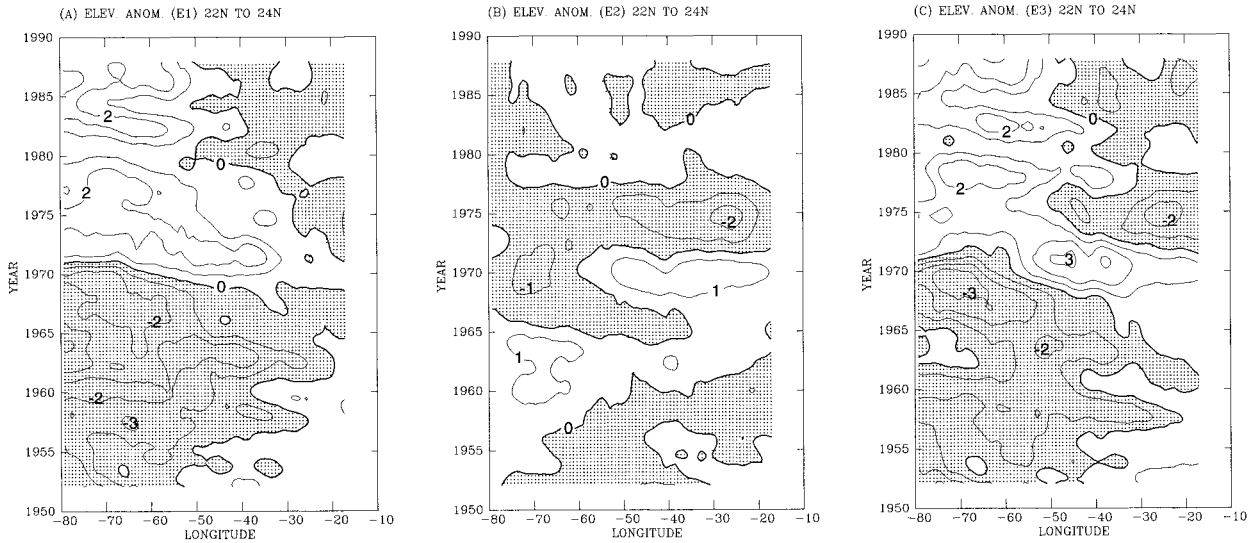

FIG. 10. As in Fig. 8 but for 22° to 24°N.

negative anomalies prior to 1970, and positive anomalies after 1971 (Figs. 9c and 10c). The anomalies of the lower latitudes seem to affect the Gulf Stream, which shows anomalously low elevation prior to 1970 and higher after 1971, as seen in Fig. 11c; this change in the Gulf Stream is consistent with the change seen in Fig. 7. In summary, Figs. 9–12 do indicate prior to 1970, the existence of long Rossby wave–like anomalies as seen in Sturges and Hong (1995) and in Sturges et al. (1998) that seem to affect the Gulf Stream and the subtropical gyre and caused the drop in the Bermuda sea level.

The linear response of the ocean variability to the combined effect of SST and wind anomalies (Fig. 8c) and the fact that it takes several years for the anomalies to propagate across the ocean might be further exploited in future climate prediction studies. In fact, a recent study by Griffies and Bryan (1997) indicated the possible predictability of decadal oscillations using ensemble coupled model simulations. For example, can the dramatic change in the Bermuda sea level be predicted years in advance using an ocean or a coupled model when altimeter data indicate unusual surface anomalies in the eastern North Atlantic? To start investigating this possibility, the correlation between the surface elevation near Bermuda and that of all other points is calculated as

$$C(x, y, \Delta t) = \frac{\sum_n [\eta(x_B, y_B, t_n + \Delta t)\eta(x, y, t_n)]}{\left\{\sum_n [\eta(x_B, y_B, t_n + \Delta t)^2] \sum_n [\eta(x, y, t_n)^2]\right\}^{1/2}}, \quad (2)$$

where the sum is calculated over all months $n = 1, 2, \cdots, N$, during the time period 1950 to 1989 $-$ Δt. Subscript "B" signifies the Bermuda location and Δt is a time lag. Figure 13 shows examples of the correlation for lags of 8, 6, and 2 years. The 95% and 99% estimated confidence levels for these calculations correspond to correlations larger than 0.5 and 0.8, respectively. Eight years in advance (Fig. 13a), the Bermuda sea level is positively correlated with anomalies in the eastern North Atlantic (shaded regions have $C > 0.5$) at three locations, north of 40°N, around 20°N, and around 10°N. For a lag of 6 years (Fig. 13b), the three areas of largest correlations have shifted westward to around the Mid-Atlantic Ridge, indicating the westward propagation of Rossby waves discussed before; the Bermuda sea level is also highly correlated with the Gulf Stream region. For a shorter time lag (Fig. 13c), the Bermuda sea level has the highest correlations with the subtropical region east of Bermuda and with the Gulf Stream region around the south Atlantic Bight; the latter may indicate the effect of the Rossby waves in low latitude on the Gulf stream as seen in Fig. 11c. These calculations favor the possibility of predicting long-term changes in the subtropical gyre, the Gulf Stream, and coastal regions in the western North Atlantic years in advance and indicate particular regions where remote anomalies should be looked for. It should be noted, that the travel time of long Rossby waves across the basin is only about half of the time lag in Fig. 13a. However, the picture that emerges from Figs. 9–12 (and similar plots, not shown, at other latitudes) is not of a single Rossby wave propagating from the east and passing across Bermuda around 1970, but of a more complicated indirect effect. Interdecadal variations of wind stress over the eastern North Atlantic seem to cause periods of more intense westward propagating long Rossby waves at several latitudes; the accumulating response in the western North Atlantic then affects the subtropical gyre and the Gulf

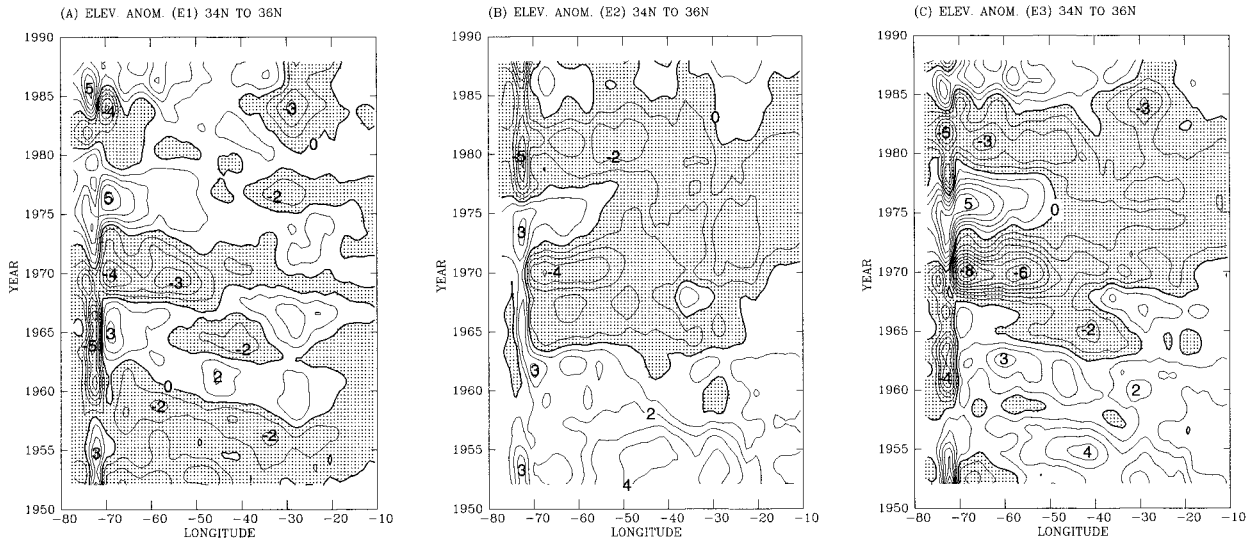

FIG. 11. As in Fig. 8 but for 34° to 36°N.

Stream, causing a delayed response at Bermuda. In a way, the Rossby waves are the mean of communication between interdecadal large-scale climatological changes in the wind pattern over the North Atlantic (Kushnir 1994) and variabilities of the subtropical gyre and the Gulf Stream.

4. Discussion and conclusions

An ocean model with a free surface, mixed layer dynamics, and bottom-following sigma coordinates has been applied to climate simulations. In a preceding paper (EM97) the model mean circulation and annual cycle were presented and compared with observations and other models. Here, the same model has been forced by monthly mean surface forcing anomalies in a series of sensitivity studies to investigate how long-term variabilities in SST and wind stress affect surface elevation and subsurface ocean variabilities, and to determine if such variabilities agree with observations. In contrast with previous diagnostic calculations such as those of Greatbatch et al. (1991) and Ezer et al. (1995) where interdecadal changes were simulated using subsurface hydrographic data, here only surface data are used in prognostic calculations in order to determine if the subsurface changes can be simulated by the model itself.

The qualitative agreement between model and observed interdecadal variabilities (Fig. 6 and Fig. 8) shows that ocean models can be useful tools to study climatic changes below the surface, given the appro-

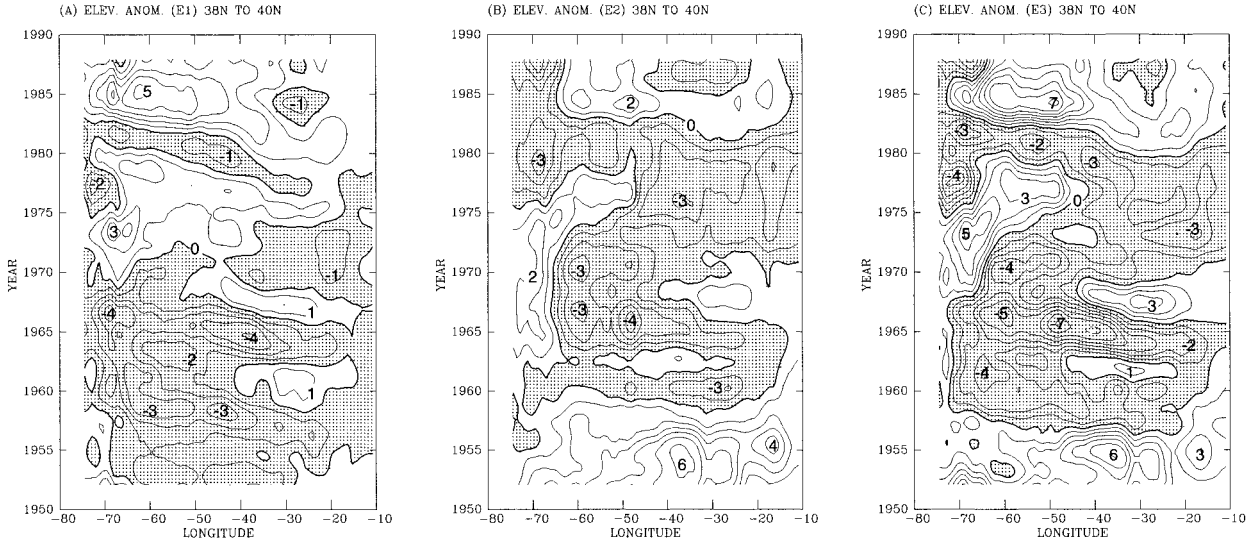

FIG. 12. As in Fig. 8 but for 38° to 40°N.

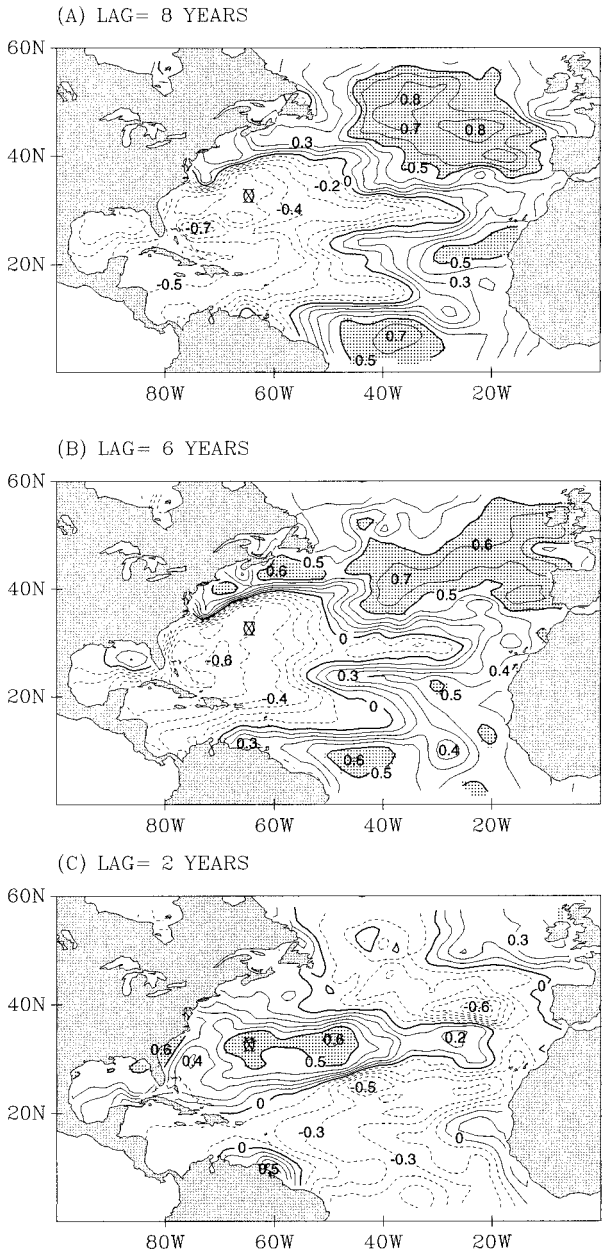

FIG. 13. Correlation between surface elevation anomaly near Bermuda (its location is indicated by "⊗") and anomalies at all other grid points at earlier time. The time lag is (a) 8 years, (b) 6 years, and (c) 2 years. Contour interval is 0.1; negative correlations are indicated by dashed contours and areas with correlations larger than 0.5 are shaded.

priate surface observations, showing that the model has the essential physics to reproduce the observed subsurface changes. However, some variabilities that involve ocean–atmosphere interaction processes can only be simulated with coupled models (e.g., Latif 1998) or with ocean models that use surface boundary conditions that include some type of an ocean–atmosphere feedback (Seager et al. 1995; Halliwell 1997, 1998).

The focus of the study was on the process of how large-scale interdecadal atmospheric variabilities affect decadal variabilities in the Gulf Stream and in the subtropical gyre. Simple wind-driven Rossby wave models (Sturges and Hong 1995; Sturges et al. 1998) as well as altimeter data (Chelton and Schlax 1996; Cipollini et al. 1997) suggest that long Rossby waves play a major role in this process. How do these waves relate to the observed variabilities in the western North Atlantic, in particular the dramatic sea level change in Bermuda during the early 1970s, and where is the preferred location to find those waves are two of the questions the simulations explain. Long Rossby wave activities can be seen in particular on the edges of the subtropical gyre, around 22°–24°N (Fig. 10) and 38°–40°N (Fig. 12); those locations also show high correlations with the Bermuda sea level signal (Fig. 13a). The tendency of such waves to be found in particular latitudes, especially in regions of enhanced zonal flows, is supported also by altimeter observations (Chelton and Schlax 1996; Cipollini et al. 1997). The westward propagation speed we find in the model (Figs. 9–12 and at other latitudes not shown) is generally comparable to that calculated by Sturges et al. (1998) from hydrographic data and that obtained from altimeter data (Chelton and Schlax 1996). For example, at the western North Atlantic the phase speed ranges between 5 and 10 cm s^{-1} at latitudes south of 20°N, 3–5 cm s^{-1} at 20°–30°N, and 2–4 cm s^{-1} north of 30°N. The scenario that emerges from these simulations is that interdecadal changes in wind patterns over the northeastern Atlantic associated with the NAO (some of them can be seen in Fig. 3) excite westward propagating long Rossby waves at several latitudes (Figs. 9–12) that affect the depth of the isotherms in the subtropical gyre (Fig. 5 and 6) and the Gulf Stream (Fig. 7). In particular, these waves, identified by negative surface elevation anomalies and uplifting isotherms, can be seen propagating toward the western North Atlantic prior to the dramatic changes that occurred in the subtropical gyre around 1970. Cold anomalies in the western North Atlantic in the early 1970s (Fig. 4a) further increase the subduction of cold water into the subsurface layers and the uplifting of the isotherms (Fig. 5).

The sensitivity experiments with different forcing indicate that there is a distinct difference between low and middle latitudes in the way the ocean responds to surface forcing on long time scales. While at low latitudes the decadal variabilities are almost solely wind driven, as suggested by Sturges and Hong (1995), at higher latitudes both SST and wind stress anomalies are important in our simulations. The experiments also show that on decadal timescales the ocean model responds in a linear fashion to the combined effect of wind stress and SST anomalies; this result and the correlation found between the subtropical sea level and sea level changes in the eastern North Atlantic years in advance are new findings

that call for further predictability studies of long-term variabilities.

Acknowledgments. We thank R. Molinari for providing us with the subsurface temperature data and W. Sturges for providing us preprints of his papers prior to publication. Comments by G. Mellor and two anonymous reviewers were most helpful to improve the manuscript. The research was supported by the NOAA's Atlantic Climate Change Program, Grant NA36GP0262, the Office for Naval Research Grant N00014-93-1-0037, and by the NOAA's Geophysical Fluid Dynamics Laboratory.

REFERENCES

Blumberg, A. F., and G. L. Mellor, 1987: A description of a three-dimensional coastal ocean circulation model. *Three-Dimensional Coastal Ocean Models*, N. Heaps, Ed., Vol. 4, Amer. Geophys. Union, 1–16.

Bryan, K., 1969: A numerical method for the study of the circulation of the world ocean. *J. Comput. Phys.,* **4,** 347–376.

Chassignet, E. P., L. T. Smith, R. Bleck, and F. O. Bryan, 1996: A model comparison: Numerical simulations of the North and equatorial Atlantic oceanic circulation in depth and isopycnic coordinates. *J. Phys. Oceanogr.,* **26,** 1849–1867.

Chelton, D. B., and M. G. Schlax, 1996: Global observations of oceanic Rossby waves. *Science,* **272,** 234–238.

Cipollini, P., D. Cromwell, M. S. Jones, G. D. Quartly, and P. G. Challenor, 1997: Concurrent altimeter and infrared observations of Rossby wave propagation near 34°N in the northeast Atlantic. *Geophys. Res. Lett.,* **24,** 889–892.

da Silva, A. M., C. C. Young, and S. Levitus, 1994: *Atlas of Surface Marine Data 1994.* Vol. 3: *Anomalies of Heat and Momentum Fluxes. NOAA Atlas NESDIS 8,* 413 pp.

Delworth, T., S. Manabe, and R. J. Stouffer, 1993: Interdecadal variations of the thermohaline circulation in a coupled ocean–atmosphere model. *J. Climate,* **6,** 1993–2011.

Ezer, T., and G. L. Mellor, 1992: A numerical study of the variability and the separation of the Gulf Stream induced by surface atmospheric forcing and lateral boundary flows. *J. Phys. Oceanogr.,* **22,** 660–682.

——, and ——, 1994: Diagnostic and prognostic calculations of the North Atlantic circulation and sea level using a sigma coordinate ocean model. *J. Geophys. Res.,* **99,** 14 159–14 171.

——, and ——, 1997: Simulations of the Atlantic Ocean with a free surface sigma coordinate ocean model. *J. Geophys. Res.,* **102,** 15 647–15 657.

——, ——, and R. J. Greatbatch, 1995: On the interpentadal variability of the North Atlantic ocean: Model simulated changes in transport, meridional heat flux and coastal sea level between 1955–1959 and 1970–1974. *J. Geophys. Res.,* **100,** 10 559–10 566.

Fu, L.-L., and D. Smith, 1996: Global ocean circulation from satellite altimetry and high-resolution computer simulation. *Bull. Amer. Meteor. Soc.,* **77,** 2625–2636.

Greatbatch, R. J., A. F. Fanning, A. D. Goulding, and S. Levitus, 1991: A diagnosis of interpentadal circulation changes in the North Atlantic. *J. Geophys. Res.,* **96,** 22 009–22 023.

Griffies, S. M., and K. Bryan, 1997: Ensemble predictability of simulated North Atlantic interdecadal climate variability. *Science,* **275,** 181–184.

Grotzner, A., M. Latif, and T. P. Barnett, 1998: A decadal climate cycle in the North Atlantic Ocean as simulated by the ECHO coupled GCM. *J. Climate,* **11,** 831–847.

Häkkinen, S., 1995: Simulated interannual variability of the Greenland Sea deep water formation and its connection to surface forcing. *J. Geophys. Res.,* **100,** 4761–4770.

Halliwell, G. R., 1997: Decadal and multidecadal North Atlantic SST anomalies driven by standing and propagating basin-scale atmospheric anomalies. *J. Climate,* **10,** 2405–2411.

——, 1998: Simulation of North Atlantic decadal/multidecadal winter SST anomalies driven by basin-scale atmospheric circulation anomalies. *J. Phys. Oceanogr.,* **28,** 5–21.

Hansen, D. V., and H. F. Bezdek, 1996: On the nature of decadal anomalies in North Atlantic sea surface temperature. *J. Geophys. Res.,* **101,** 8749–8758.

Hurrell, J. W., 1995: Decadal trends in the North Atlantic Oscillation: Regional temperature and precipitation. *Science,* **269,** 676–679.

Killworth, P. D., D. B. Chelton, and R. A. De Szoeke, 1997: The speed of observed and theoretical long extratropical planetary waves. *J. Phys. Oceanogr.,* **27,** 1946–1966.

Kushnir, Y., 1994: Interdecadal variations in North Atlantic sea surface temperature and associated atmospheric conditions. *J. Climate,* **7,** 142–157.

Latif, M., 1998: Dynamics of interdecadal variability in coupled ocean–atmosphere models. *J. Climate,* **11,** 602–624.

LeBlond, P. H., and L. A. Mysak, 1978: *Waves in the Ocean.* Elsevier, 602 pp.

Levitus, S., 1982: *Climatological Atlas of the World Ocean.* NOAA Prof. Paper No. 13, U.S. Govt. Printing Office, 173 pp.

——, 1989: Interpentadal variability of temperature and salinity at intermediate depths of the North Atlantic Ocean, 1970–1974 versus 1955–1959. *J. Geophys. Res.,* **94,** 6091–6131.

——, 1990: Interpentadal variability of steric sea level and geopotential thickness of the North Atlantic Ocean, 1970–1974 versus 1955–1959. *J. Geophys. Res.,* **95,** 5233–5238.

——, T. P. Boyer, and J. Antonov, 1994: *World Ocean Atlas 1994.* Vol. 5: *Interannual Variability of Upper Ocean Thermal Structure,* NOAA, 176 pp.

McCartney, M. S., R. G. Curry, and H. Bezdek, 1997: The interdecadal warming and cooling of Labrador Sea Water. *ACCP Notes,* IV, 1–10.

Mellor, G. L., and T. Yamada, 1982: Development of a turbulent closure model for geophysical fluid problems. *Rev. Geophys.,* **20,** 851–875.

——, and T. Ezer, 1995: Sea level variations induced by heating and cooling: An evaluation of the Boussinesq approximation in ocean model. *J. Geophys. Res.,* **100,** 20 565–20 577.

Molinari, R. L., D. A. Mayer, J. F. Festa, and H. F. Bezdek, 1997: Multiyear variability in the near-surface temperature structure of the midlatitude western North Atlantic Ocean. *J. Geophys. Res.,* **102,** 3267–3278.

New, A. L., and R. Bleck, 1995: An isopycnic model study of the North Atlantic. Part II: Interdecadal variability of the subtropical gyre. *J. Phys. Oceanogr.,* **25,** 2700–2714.

Oberhuber, J. M., 1993: Simulation of the Atlantic circulation with a coupled sea ice–mixed layer isopycnal general circulation model. Part II: Model experiment. *J. Phys. Oceanogr.,* **23,** 830–845.

Seager, R., Y. Kushnir, and M. Cane, 1995: On heat flux boundary conditions for ocean models. *J. Phys. Oceanogr.,* **25,** 3219–3230.

Semtner, A. J., 1995: Modeling ocean circulation. *Science,* **269,** 1379–1385.

Stammer, D., and C. Wunsch, 1994: Preliminary assessment of the accuracy and precision of TOPEX/POSEIDON altimeter data with respect to the large scale ocean circulation. *J. Geophys. Res.,* **99,** 24 584–24 604.

Sturges, W., and B. G. Hong, 1995: Wind forcing of the Atlantic thermocline along 32°N at low frequencies. *J. Phys. Oceanogr.,* **25,** 1706–1715.

——, ——, and A. J. Clarke, 1998: Decadal wind forcing of the North Atlantic subtropical gyre. *J. Phys. Oceanogr.,* **28,** 659–668.

Weaver, A. J., E. S. Sarachik, and J. Marotzke, 1991: Freshwater flux forcing of decadal and interdecadal oceanic variabilities. *Nature,* **353,** 836–838.